JMB

Internal Motion of Supercoiled DNA: Brownian Dynamics Simulations of Site Juxtaposition

Hongmei Jian[1], Tamar Schlick[2]* and Alexander Vologodskii[3]*

[1]*Department of Physics New York University 31 Washington Place, New York NY 10003, USA*

[2]*Department of Chemistry and Courant Institute of Mathematical Science New York University and Howard Hughes Medical Institute, 251 Mercer Street New York, NY 10012, USA*

[3]*Department of Chemistry New York University 31 Washington Place New York, NY 10003, USA*

Thermal motions in supercoiled DNA are studied by Brownian dynamics (BD) simulations with a focus on the site juxtaposition process. It had been shown in the last decade that the BD approach is capable of describing actual times of large-scale DNA motion. The bead model of DNA used here accounts for bending and torsional elasticity as well as the electrostatic repulsion among DNA segments. The hydrodynamic interaction among the beads of the model chain and the aqueous solution is incorporated through the Rotne-Prager tensor. All simulations were performed for the sodium ion concentration of 0.01 M. We first showed, to test our BD procedure, that the same distributions of equilibrium conformational properties are obtained as by Monte Carlo simulations for the corresponding DNA model. The BD simulations also predict with accuracy published experimental values of the diffusion coefficients of supercoiled DNA. To describe the rate of conformational changes, we also calculated the autocorrelation functions for the writhe and radius of gyration for the supercoiled molecules. The rate of site juxtaposition was then studied for DNA molecules up to 3000 bp in length. We find that site juxtaposition is a very slow process: although accelerated by a factor of more than 100 by DNA supercoiling, the times of juxtaposition are in the range of ms even for highly supercoiled DNA, about two orders of magnitude higher than the relaxation times of writhe and the radius of gyration for the same molecules. By inspecting successive simulated conformations of supercoiled DNA, we conclude that slithering of opposing segments of the interwound superhelix is not an efficient mechanism to accomplish site juxtaposition, at least for conditions of low salt concentration. Instead, transient distortions of the interwound superhelix, followed by continuous reshaping of the molecule, contribute more significantly to site juxtaposition kinetics.

© 1998 Academic Press

Keywords: DNA supercoiling; Brownian dynamics; kinetics of site juxtaposition; DNA dynamics; DNA topology

*Corresponding authors

Introduction

Bringing two or more specific DNA sites into close contact, or site juxtaposition, is important for many biological processes. Joining the juxtaposed sites by protein bridges occurs in many cases of transcription regulation (reviewed by Bellomy & Record, 1990; Gralla, 1996; Hochschild & Ptashne, 1986; Rippe *et al.*, 1995; Schleif, 1992; Tjian & Maniatis, 1994), site-specific recombination (Stark & Boocock, 1995; Wasserman & Cozzarelli, 1986),

and transactions of type II topoisomerases (Wang, 1996). Thus it is important to determine quantitative features of the juxtaposition process. It is particularly valuable to establish how DNA supercoiling affects the equilibrium and dynamic properties of juxtaposition because such information can lead to a better understanding of enzymatic mechanisms in systems where the reaction efficiency depends strongly on the supercoiling of the DNA substrate (Kanaar & Cozzarelli, 1992; Menzel & Gellert, 1994).

It has been shown by computer simulation that DNA supercoiling increases the equilibrium probability of site juxtaposition (Vologodskii *et al.*, 1992; Vologodskii & Cozzarelli, 1996). For highly supercoiled DNA, this increase can exceed two orders of

magnitude. It was also found that supercoiling dramatically changes the relative orientation by which two specific sites come together, shifting the maximum and reducing the width of the angular distribution (Vologodskii & Cozzarelli, 1996). These results suggest a large effect of supercoiling on juxtaposition dynamics.

The kinetics of site juxtaposition in supercoiled DNA is a challenging area for both experimental and theoretical studies. A pioneering experimental approach to the problem was developed by Parker & Halford (1991). These authors exploited competition between two closely related recombination systems where each system had specific target sites located in one circular DNA 5 kb in length. This approach was recently developed further by applying a rapid-reaction quench-flow device to the same system (Oram *et al.*, 1997). According to the data obtained, the synapsis times for the resolvase recombination system spanned a large range, from 10 ms to 100 seconds. Theoretical analysis suggested, however, that a rearrangement of non-productive DNA-protein complexes explains the slow synapsis in a subset of DNA molecules (Sessions *et al.*, 1997). The system may be too complex to extract accurate quantitative information about the kinetics of site juxtaposition.

Theoretical analysis of site juxtaposition kinetics in relaxed circular DNA was first described by Berg (1984), who estimated polymer cyclization time. However, as his analysis contains several assumptions, the accuracy obtained has yet to be established. Recent simulation data for cyclization kinetics are in some disagreement with Berg's results (Podtelezhnikov & Vologodskii, 1997) and it is hardly possible to extend this kind of approach to supercoiled DNA. Marko & Siggia (1995) applied a simple reptation model to analyze the dynamics in supercoiled DNA. They concluded that for supercoiled molecules the rate of the juxtaposition is inversely proportional to the third power of DNA length; therefore, juxtaposition would be very slow for molecules longer than a few kb in length. However, their theoretical analysis did not account for branching and other irregularities of supercoiled conformations. Recently, Marko formulated another phenomenological model which considered branching effects (Marko, 1997) and found that in this case the juxtaposition time would be proportional to the square of the DNA length. In general, all theoretical approaches to site juxtaposition dynamics in supercoiled DNA must use different assumptions to simplify the problem considerably. At the same time, the problem is well suited for computer simulations. Elaborate models of DNA and tested computational procedures make dynamic simulations a powerful tool for these types of kinetic problems.

Several approaches were developed recently to simulate dynamic properties of supercoiled DNA (Tan & Harvey, 1989; Schlick & Olson, 1992; Chirico & Langowski, 1994; Schlick, 1995). One of these approaches, based on BD (Ermak & McCammon, 1978), is most suitable to study the slow process of site juxtaposition. It has been shown that BD allows accurate quantitative description of both equilibrium and transport properties of DNA molecules (Allison *et al.*, 1989, 1990; Allison, 1986; Chirico & Langowski, 1992, 1994). Furthermore, conformational changes over large time intervals can be simulated. Here we use BD simulations to study the dynamics of site juxtaposition in supercoiled DNA.

We have recently developed a DNA model for BD simulations of linear DNA molecules which was carefully tested against available experimental and simulation data (Jian *et al.*, 1997). Although basic features of the model are similar to those of the Allison and Langowski groups (Allison *et al.*, 1989, 1990; Chirico & Langowski, 1996; Heath *et al.*, 1996; Hammermann *et al.*, 1997) some details, such as the electrostatic interaction among DNA segments, are treated differently. We also improved performance of the BD algorithm so that longer trajectories can be simulated for the same accuracy and computer time. Here we describe the model's extension, along with the computational procedure, to closed circular DNA, and report on simulations of site juxtaposition in supercoiled molecules. This is the first application of BD simulations, to our knowledge, for studying this important biological problem.

Results

We began by simulating equilibrium thermal motion of supercoiled DNA for circular molecules 600–3000 bp in length. Each production run started from a randomly chosen conformation from a generated equilibrium set. This initial set was constructed by Monte Carlo (MC) simulations or by preliminary BD runs started from regular polygon shapes. Typical equilibrium conformations of supercoiled DNA are rather irregular at low superhelix density ($|\sigma| < 0.02$) but adopt interwound superhelices at higher degrees of supercoiling (Vologodskii & Cozzarelli, 1994). We will return to this issue later when we analyze the simulated rate constants of site juxtaposition.

Before presenting results for site juxtaposition dynamics, we report on tests of our computational procedure by comparing some results of dynamic simulations with corresponding equilibrium properties obtained by MC simulations and with available experimental data. Such comparisons are possible because the thermal ensembles generated by a long BD run must correspond the equilibrium distribution of conformations (Ermak & McCammon, 1978).

Tests of the computational procedure

We first compare equilibrium distributions of the radius of gyration, R_g, and writhing number, Wr, obtained by BD and MC simulations. The same DNA model was used in both cases. Figure 1
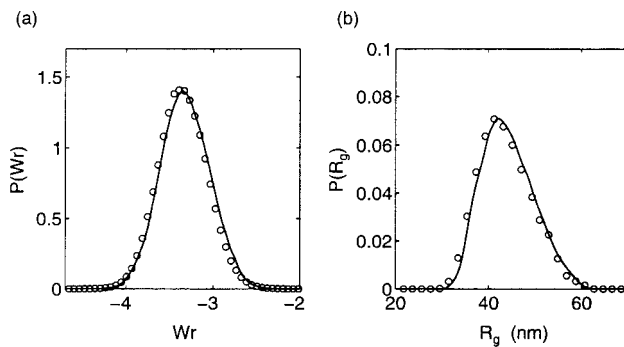
Figure 1. Comparison of the equilibrium conformational properties of supercoiled DNA simulated by the BD and MC procedures. The distribution functions of writhe (a) and the radius of gyration (b) were calculated for supercoiled DNA of 1500 bp with $\sigma = -0.06$. Both the MC results (continuous lines) and the BD data ($\bigcirc$) were obtained for the same DNA model.

shows the results for model chains corresponding to closed circular DNA chains of 1500 bp with $\sigma = -0.06$. We note an excellent agreement between the two methods for both properties. Similar results were obtained for other values of σ. It has been shown that the DNA model used here provides very good predictions of the experimentally observed equilibrium properties of supercoiled DNA (Rybenkov *et al.*, 1997a,b).

We next compare translational diffusion coefficients of supercoiled DNA obtained by BD, D^{BD}, with values available from experiment, D^{exp}. The values D^{BD} were calculated from the displacement of the center of mass of the model chains, $\mathbf{r}(t)$, according to the Einstein-Stokes equation:

$$6tD = \langle |\mathbf{r}(t) - \mathbf{r}(0)|^2 \rangle \qquad (1)$$

for sufficiently long time, t. We found in our studies of long linear DNA, that t of about 1 μs provides well converged values of D^{BD} (Jian *et al.*, 1997). Better statistics are obtained by analyzing multiple trajectories, each of about 10 ms in length, for each set of DNA length and σ. The good agreement between the simulated data and published experimental results can be seen from Table 1.

Table 1. Translation diffusion coefficients of supercoiled DNA obtained by BD simulations *versus* experimental measurements

DNA length (bp)	D^{BD}, $\sigma = -0.03$	D^{BD}, $\sigma = -0.06$	D^{exp} [a]
2000	5.5 ± 0.1	5.9 ± 0.15	6.0
3000	5.3 ± 0.1	4.7 ± 0.15	4.6

[a] The experimental values were obtained by interpolation of the straight line in Figure 3 of Langowski & Giesen (1989). The values of the superhelix densities for these data are not known, but are likely to be close to −0.06, the typical value *in vivo*. All values of D are in units of 10^{-8} cm^2 s^{-1}.

Relaxation times of supercoiled DNA

Since our focus is on the thermal motion of supercoiled DNA molecules, and mean properties do not change on average throughout the simulated trajectories, it is appropriate to describe chain dynamics in terms of autocorrelation functions. An autocorrelation function for a conformational variable A, $c_A(t)$, is defined as:

$$c_A(t) = \frac{\langle A(t)A(0) \rangle - \langle A \rangle^2}{\sigma_A^2} \qquad (2)$$

where the brackets ($\langle \ \rangle$) correspond to an averaging over all possible trajectories in conformational space, and σ_A^2 is the variance of A. Note that $c_A(0)$ is equal to 1 and $c_A(t) \rightarrow 0$ as $t \rightarrow \infty$ since $A(t)$ and $A(0)$ become uncorrelated. The rate of decay of $c_A(t)$ describes how long a system retains prior information.

Figure 2 shows the autocorrelation functions for Wr and R_g of supercoiled DNA, $c_W(t)$ and $c_R(t)$. We note that the functions do not have a linear form in semilogarithmic coordinates and thus cannot be described by a single-exponent decay function. However, the single exponential approximation for $c_A(t)$:

$$c_A(t) \propto \exp(-t/\tau_A) \qquad (3)$$

where τ_A is a constant, is good for large t. The major (largest) relaxation time for Wr and R_g, τ_W and τ_R, respectively, can then be determined from the Figure unambiguously. The values of τ_W and τ_R calculated as a function of σ are shown in Figure 3. Although both the writhe and the radius of gyration are global conformational properties, they exhibit very different relaxation features. Values of τ_W are reduced by a factor of 5 as $|\sigma|$ increases from zero to 0.06, while of τ_R is independent of the supercoiling level within the accuracy of our computations. Both τ_W and τ_R increase as a function of DNA length (Figure 4).

For additional tests of our simulation procedure, we calculated the optical anisotropy decay, $B(t)$, for a closed chain 196 bp in length, repeating the
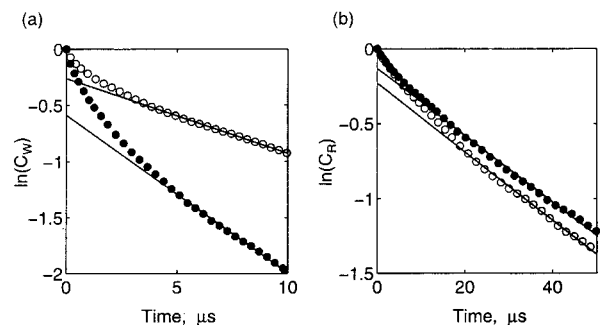

Figure 2. Autocorrelation functions for the writhe (a) and radius of gyration (b) of supercoiled DNA. The results of BD simulations correspond to DNA molecules 1500 bp in length, for two $|\sigma|$ values: 0.03 ($\bigcirc$) and 0.06 ($\bullet$).
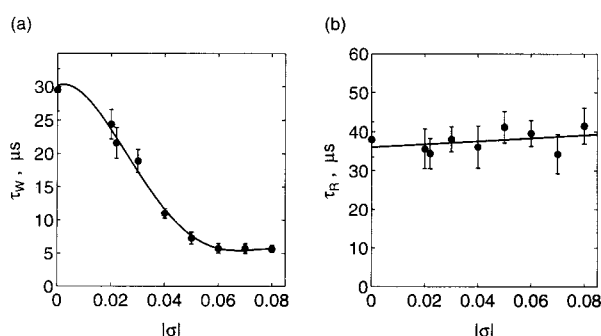
Figure 3. The largest relaxation times for writhe (a) and the radius of gyration (b) of supercoiled DNA as functions of the superhelix density. Results of BD simulations for DNA 1500 bp in length (●) are shown. Error bars correspond to one standard deviation.

Table 2. Computational cost of our BD simulations of supercoiled DNA

DNA length (bp)	Simulation length (ms)	CPU time (days)[a]
600	0.22	0.02
1500	3.4	2.0
3000	12	40

[a] CPU time is calculated on one 175-MHZ R10000 processor of a Silicon Graphics Power Challenge machine.

result of Heath *et al.* (1996). After adjusting our DNA model and parameters to those used by Heath *et al.* (1996), we found no difference, within the statistical error of the simulations, between our results and their data.

Rate of site juxtaposition

We compute the average time of a first collision, $\langle \tau_c \rangle$, between two sites separated along the chain contour by a distance L_s. That is, we designate an interbead separation, and consider a collision when the distance between their centers is less than some critical value r_0. The value $r_0 = 10$ nm was used throughout this work, relevant to a the size of large protein-DNA complexes. This relatively large value of r_0 accelerated our very time-consuming calculations (see Table 2 for computational requirements). Clearly, the computed times $\langle \tau_c \rangle$ depend on the chosen r_0. For linear or relaxed circular chains, $\langle \tau_c \rangle$ is inversely proportional to r_0 (Podtelezhnikov & Vologodskii, 1997). A weaker dependence should be expected for supercoiled DNA molecules. This is because tight confor-

mations of supercoiled DNA restrict its motion (Schlick & Olson, 1994). Hence two juxtaposed sites stay near each other a long tune and intensively sample the range of short distances between them before they move apart.

Our reported value of $\langle \tau_c \rangle$ represents an average over all bead pairs separated by a particular distance. Thus we continue a simulation until all pairs of beads that are L_s bp apart collide within our definition. To reduce statistical error, several trajectories were performed for each value of chain length and supercoiling.

Figure 5 shows the distribution of τ_c for a model chain 1500 bp in length and $\sigma = -0.06$. The distribution is far from a simple exponentially decaying function; the probability of having a particular τ_c diminishes rapidly for $\tau_c < \langle \tau_c \rangle$ (about 0.5 ms here) but much slower for $\tau_c > \langle \tau_c \rangle$. This differs from linear or relaxed circular DNA where the distribution can be approximated by a single exponent with very high accuracy (Wilemski & Fixman, 1974; Podtelezhnikov & Vologodskii, 1997). This non-exponential distribution of τ_c makes computation
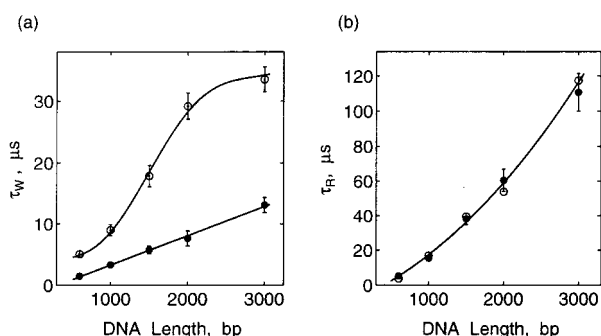

Figure 4. The largest relaxation times for writhe (a) and the radius of gyration (b) as functions of the length of supercoiled DNA. Results of BD simulations are shown for $|\sigma| = 0.03$ (○) and $|\sigma| = 0.06$ (●), and error bars correspond to one standard deviation.
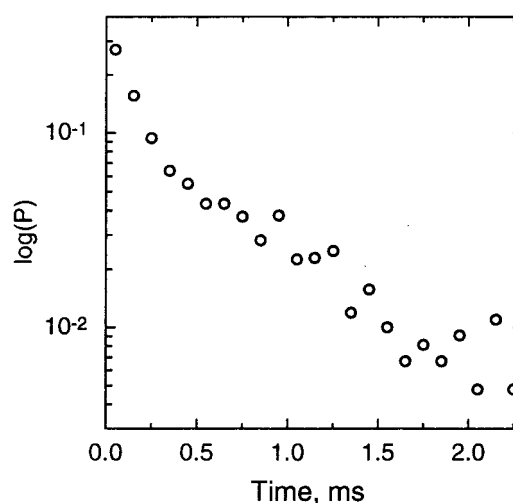

Figure 5. The distribution of the first collision time (see the text) for sites separated by 300 bp along the DNA contour. The data correspond to BD simulations for supercoiled DNA 1500 bp in length, with $|\sigma| = 0.06$. The fraction of collisions, P, which occured in the time interval of 0.1 ms is plotted as a function of time. The data clearly show that the distribution cannot be approximated by a single exponent.
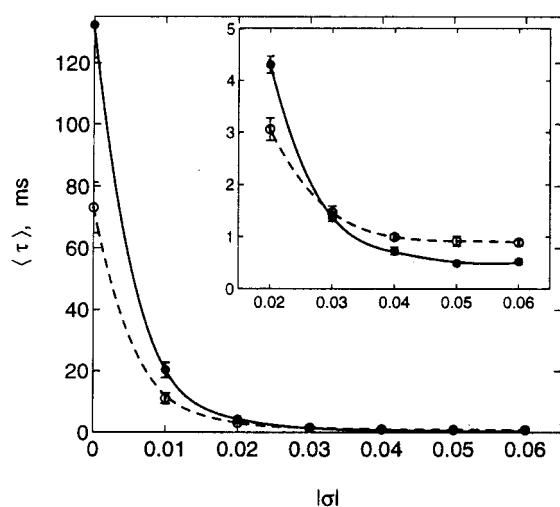
Figure 6. The average collision time of two sites as a function of DNA superhelix density. The simulation results were obtained for supercoiled DNA 1500 bp in length, with site separation along the contour of 300 bp (●) and 600 bp (○). The error bars are shown only when they are larger than the circle size and correspond to one standard deviation. The inset enlarges the data for a shorter range of time.

of $\langle \tau_c \rangle$ even more time consuming. We have therefore reliably estimated $\langle \tau_c \rangle$ only for supercoiled molecules shorter than 3000 bp.

The values of the average collision time for sites separated by 300 and 600 bp in 1500 bp DNA are shown in Figure 6. Firstly, we see from the Figure that even for very short closed DNA chains the values of $\langle \tau_c \rangle$ are in the ms range. Site juxtaposition is a very slow process: the values of $\langle \tau_c \rangle$ exceed the relaxation times τ_W and τ_R by factors of 100–1000 (compare with Figure 2). Secondly, supercoiling affects $\langle \tau_c \rangle$ greatly. The values of $\langle \tau_c \rangle$ are about 100 times larger for relaxed DNA than for highly supercoiled model chains. Thirdly, relatively small differences are seen for two different values of L_s.

For relaxed DNA, we found that $\langle \tau_c \rangle$ values can well exceed 100 ms. Thus very long trajectories are necessary for accurate determination of $\langle \tau_c \rangle$. For relaxed DNA 1500 bp in length we were able to produce only one trajectory of 206 ms in length which already took about four months of CPU time (see Table 2). Only 83% of the selected sites with $L_s = 300$ bp and 95% of the selected sites with $L_s = 600$ bp have collided during this run. Therefore, the statistical error is rather large in this case.

Figure 7 shows the effect of DNA length, L, on the rate of site juxtaposition. Data are shown for supercoiled molecules with $\sigma = -0.03$ and $\sigma = -0.06$ where $\langle \tau_c \rangle$ is not too large. Although the statistical error is rather large for chain lengths of 2000 and 3000 bp, the data show very weak DNA-length dependence of $\langle \tau_c \rangle$ for $L > 2000$ bp for physiological superhelical densities.

Site juxtaposition and internal motions in supercoiled DNA

Dynamic simulations open opportunities for examining the kind of internal motions that contribute to site juxtaposition. Selected successive conformations along a simulation for 3000 bp, $\sigma = -0.06$ are shown in Figure 8. Two points on the chain, separated by 1200 bp, are indicated by open and filled arrows, and were selected at the onset. The time interval separating successive conformations is about 100 μs, or one seventh of the average time of the first collision for this DNA length and σ (see Figure 7). We note that the superhelix changes significantly in shape during this interval, including the number of superhelix branches. During the first 700 μs, however, the superhelix retains an unbranched conformation and thus the displacement of the marked points is rather small. The first collision of the points took place only around $t = 4.2$ ms, following many global changes of the superhelix conformation. From these and other similar data we conclude that large-scale arrangements of superhelical conformations are very important for site juxtaposition, perhaps more so than the relative slithering of segments along the contour of the interwound superhelix (Benjamin & Cozzarelli, 1986).

Discussion

In this work we began to explore, using BD simulations, kinetic features of supercoiled DNA. We considered thermal motions of molecules around equilibrium rather than pathways to equilibrium. Throughout these simulations, many conformational rearrangements can be followed but no systematic changes in equilibrium confor-
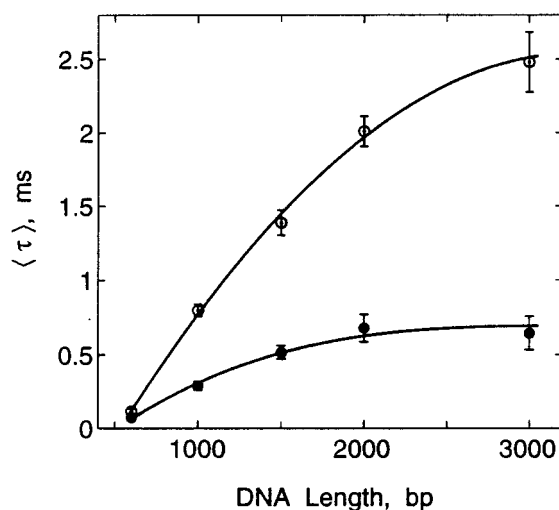

Figure 7. Dependence of the average time of juxtaposition of two sites on the length of supercoiled DNA. The DNA superhelix density is equal to −0.03 (○) and −0.06 (●), and the site separation along the DNA contour is 600 bp.
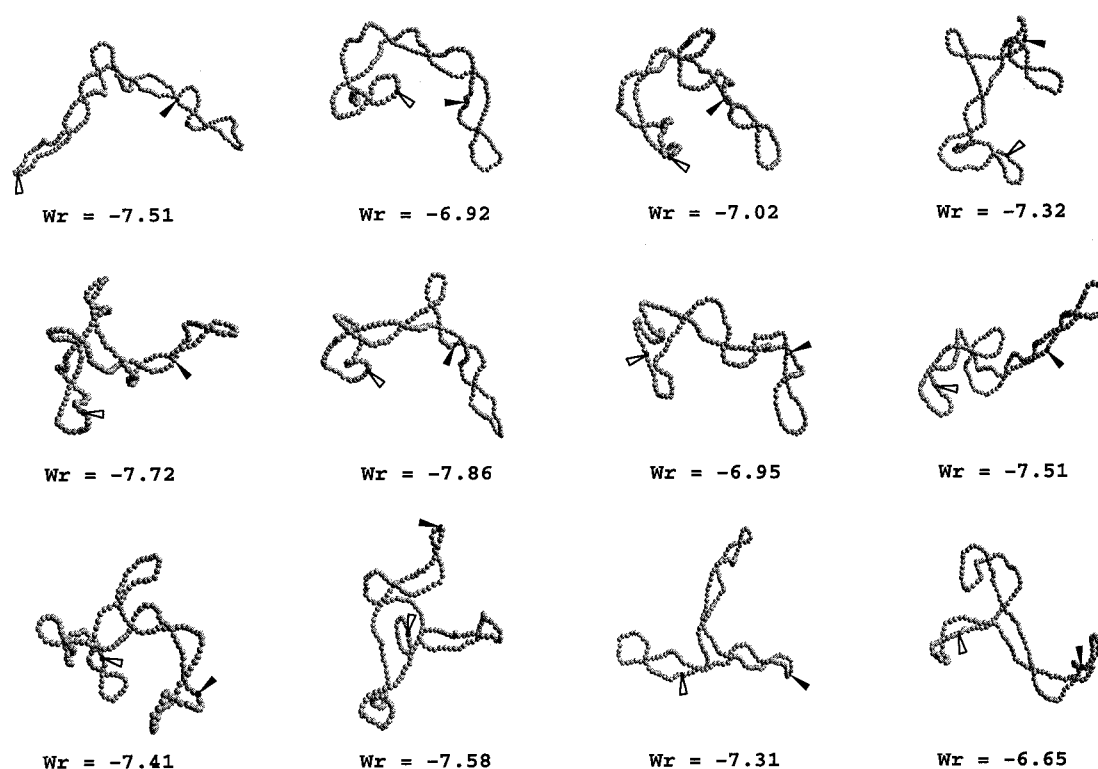
Figure 8. Snapshots of the supercoiled DNA conformations. The data correspond to DNA 3000 bp in length, with $|\sigma| = 0.06$. The value of *Wr* is shown for each conformation. Successive snapshots are separated by 100 μs. Two sites marked by open and filled arrows are 1200 bp away along the contour and were arbitrarily chosen at the beginning of the simulation. The first collision of the selected sites took place at $t = 4.2$ ms.

mational properties are involved. One of the basic questions about such processes is how long the molecules "remember" their previous conformations. Autocorrelation functions were used to study this question quantitatively. Our results show that characteristic times for retaining memory with regards to the writhe and the radius of gyration of supercoiled DNA are in the range of tens of μs for supercoiled DNA up to 3000 bp in length.

We focused on the biologically relevant dynamic process of site juxtaposition in long DNA. This property is important for a quantitative understanding of many enzymatic reactions involving two or more DNA sites separated along the chain contour. We found that site juxtaposition is a very slow process and is accelerated by a factor of more than 100 by DNA supercoiling. The increase of the average time of juxtaposition, $\langle \tau_c \rangle$, by two orders of magnitude *via* DNA supercoiling matches the similar increase of the equilibrium probability of site juxtaposition (Vologodskii & Cozzarelli, 1996). However, even for highly supercoiled DNA the times of juxtaposition were in the range of ms, about two orders of magnitude higher than the relaxation times of writhe and the radius of gyration for the same molecules. The value of $\langle \tau_c \rangle$ is clearly larger for longer DNA molecules. Therefore, *in vivo*, DNA must have developed mechanisms to

reduce $\langle \tau_c \rangle$. DNA supercoiling, in particular, may be one possible route to increase the rate of the juxtaposition. Protein looping and anchoring are other possible ways and can act in addition to supercoiling.

By inspecting successive simulated conformations of supercoiled DNA, we conclude that slithering of opposing segments of the interwound superhelix is not an efficient way to accomplish site juxtaposition in general. Transient distortions of the interwound superhelix, followed by global reshaping of the molecule, contribute more significantly to site juxtaposition kinetics. This reshaping of superhelical conformations changes the branching patterns of the molecule and makes possible large-scale changes of the intersite distances in a short period of time. A similar conclusion was recently reached by Chirico & Langowski (1996).

Although we found that the juxtaposition time increases with DNA length (Figure 7) and with the site separation along the DNA contour, our data pertain only to plasmids up to 3000 bp in length. This limitation is due to the high cost of computer time for BD simulations with hydrodynamics. In addition, simulations were performed for a low concentration of sodium ions, 0.01 M. It is known, however, that conformations of supercoiled DNA are less regular at these ionic conditions than at higher physiological values (Vologodskii, 1992;

Vologodskii & Cozzarelli, 1994; Schlick *et al.*, 1994; Rybenkov *et al.*, 1997a,b) and this difference can affect the dynamic properties of supercoiled DNA. Simulations for higher concentrations of sodium ions are more demanding computationally because accounting accurately for the electrostatic interaction requires finer resolution. Future studies that combine algorithmic and technological improvements are required to overcome these practical limitations.

The only experimental approach to study the rate of site juxtaposition was developed by Halford and co-workers (Oram *et al.*, 1997; Parker & Halford, 1991) who measured the rate of synapsis of two DNA-protein complexes in the resolvase system of site-specific recombination. Keeping well in mind the difference in ionic conditions between our simulation and these experimental studies, for example magnesium ions which strongly affect conformations of supercoiled DNA (Rybenkov *et al.*, 1997a,b) were included into the experimental system, we can only attempt a rough comparison of the results. Oram *et al.* (1997) found that the time of synapsis extends over six orders of magnitude, from a few ms to thousands of seconds. The distribution of the synapsis time did not change by doubling DNA size and by changing the separation between the *res* sites along the chain contour. Although we also found a rather weak length dependence for the juxtaposition time (see Figure 7), there is large disagreement regarding values of the juxtaposition time between our simulations and the experimental data. According to the simulation results for supercoiled DNA 1500 bp in length, 25% of designated pairs collide first during 0.1 ms, with the next 70% colliding during 2 ms. Thus, the essential part of the distribution of $\langle \tau_c \rangle$ only covers about two orders of magnitude. It is highly unlikely that the difference in DNA lengths used in the simulation and experiment is responsible for such a difference between the measured and simulated collision times. We believe that our data confirm the basic conclusion of Sessions *et al.* (1997) that some slow restructuring of the DNA-protein complexes, or an additional process, must explain the long times of synapsis observed by Oram *et al.* (1997).

DNA Model and Methods of Calculations

DNA model

Our DNA model is based on the discrete worm-like chain similar to one developed by Allison *et al.* (Allison *et al.*, 1989; Allison, 1986; Allison & McCammon, 1984) and extended later by Chirico & Langowskii for the case of supercoiled DNA (Chirico & Langowski, 1994, 1996). A careful adaptation, parameterization and testing for linear DNA was described by Jian *et al.* (1997).

A DNA molecule composed of n Kuhn statistical lengths is modeled as a closed chain of kn straight elastic segments of equilibrium length l_0. To specify the torsional deformation of the chain, the body-fixed co-ordi-
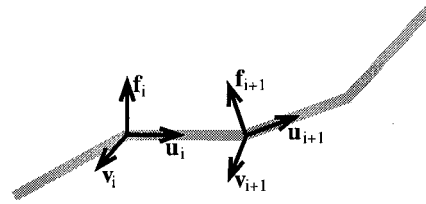

Figure 9. The DNA model. The body-fixed co-ordinate frame defined by the unit vectors $\mathbf{f}_i$, $\mathbf{v}_i$, $\mathbf{u}_i$ is attached to each vertex of the chain to specify the torsional deformation of the chain.

nate (bfc) frame defined by the unit vectors $\mathbf{f}_i$, $\mathbf{v}_i$, $\mathbf{u}_i$ is attached to each vertex of the chain (Figure 9). The chain energy consists of the following four terms.

The stretching energy is computed as:

$$E_s = \frac{h}{2}\sum_{i=1}^{nk}(l_i - l_0)^2 \qquad (4)$$

where l_i is the actual length of segment i, and h is the stretching rigidity constant. The energy E_s is considered as a computational device rather than an attempt to account for the actual stretching elasticity of the double helix. Smaller values of h allow larger timesteps in the BD simulations, but also imply larger departures from l_0 (Jian *et al.*, 1997). We chose $h = 100\ k_BT/l_0^2$, where k_BT is the Boltzmann factor so that the variance of l_i is close to $l_0^2/100$ for this value of h.

The bending energy, E_b, is specified by angular displacements θ_i of each segment i relative to segment $i + 1$:

$$E_b = \frac{g}{2}\sum_{i=1}^{kn}\theta_i^2 \qquad (5)$$

The bending rigidity constant g is defined so that the Kuhn statistical length corresponds to k rigid segments (Frank-Kamenetskii *et al.*, 1985). It was shown previously that equilibrium properties of supercoiled conformations do not change, within the accuracy of the simulations, if $k \geqslant 10$ (Vologodskii *et al.*, 1992). We use $k = 20$ in this work; this corresponds to $g = 9.82\ k_BT$ and $l_0 = 5$ nm when using 100 nm for the Kuhn length (Hagerman, 1988).

The energy of electrostatic intersegment interaction is specified by the Debye-Hückel potential as a sum over all pairs of point charges located at the chain vertices:

$$E_e = \frac{\nu^2 l_0^2}{D}\sum_{j>i+1}^{nk}\frac{\exp(-\kappa r_{ij})}{r_{ij}} \qquad (6)$$

In this expression, ν is the effective linear charge density of the double helix, D is the dielectric constant of water, r_{ij} is the distance between vertices i and j, and $1/\kappa$ is the Debye length. This system of point charges located at the vertices represents a good approximation to continuous charges if the length l_0 is sufficiently small (Vologodskii & Cozzarelli, 1995). The value, ν, corresponds to the solution of the Poisson-Boltzmann equation for DNA modeled as a charged cylinder. It was found by Stigter (1977) that this solution can be approximated well by the Debye-Hückel potential. This approximation requires only a suitable definition of ν to match the potential-distance curve in the overlap region far from the cylindrical surface. All calculations here correspond to 10 mM of

NaCl; for these ionic conditions $1/\kappa = 3.03$ nm and $\nu = 2.43$ e/nm.

In addition to these three terms present in the model of linear DNA (Jian *et al.*, 1997), the energy of torsional deformations is included following the work of Chirico & Langowski (1994). Namely, Euler angles $\alpha_{i,i+1}$, $\beta_{i,i+1}$, $\gamma_{i,i+1}$ were used to describe the transformation from the bfc frame i to $i+1$. In this representation, $\beta_{i,i+1}$ is the bending angle, θ_i. The torsional angle between frames i and $i+1$ is defined as:

$$\phi_{i,i+1} = \alpha_{i,i+1} + \gamma_{i,i+1} \qquad (7)$$

Thus the torsional energy is expressed as:

$$E_t = \frac{C}{2l_0} \sum_{i=1}^{kn} (\alpha_{i,i+1} + \gamma_{i,i+1} - \phi^0)^2 \qquad (8)$$

where C is the DNA torsional rigidity constant, and ϕ^0 is the equilibrium twist of one model segment. The angle ϕ^0 is given by:

$$\phi^0 = 2\pi l_0/\gamma \qquad (9)$$

where γ is the DNA helical repeat, equal to 3.55 nm (Peck & Wang, 1981). The value of C is set to 2×10^{-19} erg cm (Hagerman, 1988).

To account for hydrodynamic interactions of DNA in solution we assume that beads are located at each vertex of model chain. It is important to emphasize that the only interaction involving beads *per se* is hydrodynamics. Thus the presence of the beads does not affect equilibrium properties of the model chain. We use the Rotne-Prager diffusion tensor (Rotne & Prager, 1969) to specify the hydrodynamic interaction, as:

$$\mathbf{D}_{ii} = \frac{k_B T}{6\pi\eta a} \mathbf{I}$$

$$\mathbf{D}_{ij} = \frac{k_B T}{8\pi\eta r_{ij}} \left[\left(\mathbf{I} + \frac{\mathbf{r}_{ij}\mathbf{r}_{ij}}{r_{ij}^2} \right) + \frac{a^2}{2r_{ij}^2} \left(\frac{1}{3}\mathbf{I} - \frac{\mathbf{r}_{ij}\mathbf{r}_{ij}}{r_{ij}^2} \right) \right]$$

$$i \neq j \qquad (10)$$

where η is the solvent viscosity, $\mathbf{I}$ is 3×3 identity tensor, r_{ij} specifies the interparticle distance, and the inter-bead vector $\mathbf{r}_{ij} = \mathbf{r}_i - \mathbf{r}_j$. The hydrodynamic radius, a, is set to 1.78 nm to yield known values of translational diffusion coefficients as a function of DNA length (Jian *et al.*, 1997).

Brownian dynamics simulations

We used the second-order BD algorithm (Iniesta & Garcia de la Torre, 1990) in which the chain displacement during a time interval Δt is calculated in two steps. If $\mathbf{r}_i^n$ is a current position of bead i, an auxiliary position of the bead, $\tilde{\mathbf{r}}_i^{n+1}$, is calculated according to the first-order algorithm of Ermak & McCammon (1978):

$$\tilde{\mathbf{r}}_i^{n+1} = \mathbf{r}_i^n + \frac{\Delta t}{k_B T} \sum_j \mathbf{D}_{ij}^n \mathbf{F}_j^n + \mathbf{R}_i^n \qquad (11)$$

Here $\mathbf{F}_j^n$ is the direct force acting on bead j, and $\mathbf{R}_i^n$ is a vector of Gaussian random numbers of zero mean and covariance matrix:

$$\langle \mathbf{R}_i^n \mathbf{R}_j^n \rangle = 2\mathbf{D}_{ij}^n \Delta t \qquad (12)$$

The procedure described by Ermak & McCammon (1978) is used to generate the components of $\mathbf{R}_i^n$. The

values $\tilde{\mathbf{r}}_i^{n+1}$ are then used for the second step of the algorithm to generate the final position:

$$\mathbf{r}_i^{n+1} = \mathbf{r}_i^n + \frac{\Delta t}{2k_B T} \sum_j (\mathbf{D}_{ij}^n \mathbf{F}_j^n + \tilde{\mathbf{D}}_{ij}^{n+1} \tilde{\mathbf{F}}_j^{n+1}) + \tilde{\mathbf{R}}_i^{n+1} \qquad (13)$$

where

$$\langle \tilde{\mathbf{R}}_i^{n+1} \tilde{\mathbf{R}}_j^{n+1} \rangle = (\mathbf{D}_{ij}^n + \tilde{\mathbf{D}}_{ij}^{n+1}) \Delta t \qquad (14)$$

Here $\tilde{\mathbf{F}}_j^{n+1}$ and $\tilde{\mathbf{D}}_{ij}^{n+1}$ are calculated using the values of $\tilde{\mathbf{r}}_i^{n+1}$.

While the second-order algorithm provides better accuracy, it doubles CPU time as well. To improve the computational performance we modified the algorithm by eliminating calculation of $\tilde{\mathbf{D}}_{ij}^{n+1}$ and $\tilde{\mathbf{R}}_i^{n+1}$ in the second phase, so that the previous values, $\mathbf{D}_{ij}^n$ and $\mathbf{R}_i^n$, are re-used at the second substep. We found that this modification does not affect the accuracy of calculations while reducing CPU time by a factor of nearly 2 (Jian *et al.*, 1997). By testing many equilibrium and dynamic properties, we found that a further reduction of CPU time can be achieved if the tensor $\mathbf{D}_{ij}^n$ is only updated every ten timesteps. This produces roughly the same numerical accuracy as the second-order method while reducing the average CPU time per timestep by another factor of four.

At each timestep Δt, the beads and the associated coordinate frames also rotate around the local axis of each segment. The torsional deformation of the chain was treated as described by Allison *et al.* (1989).

We found earlier that the timestep $\Delta t = 600$ ps can be used for our model with the modified second-order algorithm (Jian *et al.*, 1997). This is the value used throughout these computations.

References

Allison, S. A. (1986). Brownian dynamics simulation of wormlike chains. Fluorescence depolarization and depolarized light scattering. *Macromolecules*, **19**, 118–124.

Allison, S. A. & McCammon, J. A. (1984). Multistep Brownian dynamics: application to short wormlike chains. *Biopolymers*, **23**, 363–375.

Allison, S., Austin, R. & Hogan, M. (1989). Bending and twisting dynamics of short DNAs. Analysis of the triplet anisotropy decay of a 209 base pair fragment by Brownian simulation. *J. Chem. Phys.* **90**, 3843–3854.

Allison, S. A., Sorlie, S. S. & Pecora, R. (1990). Brownian dynamics simulations of wormlike chains – dynamic light scattering from a 2311 base pair DNA fragment. *Macromolecules*, **23**, 1110–1118.

Bellomy, G. R. & Record, M. T., Jr (1990). Stable DNA loops *in vivo* and *in vitro*: roles in gene regulation at a distance and in biophysical characterization of DNA. *Prog. Nucl. Acid Res. Mol. Biol.* **39**, 81–128.

Benjamin, H. W. & Cozzarelli, N. R. (1986). DNA-directed synapsis in recombination: Slithering and random collision of sites. In *Genetic Chemistry: The Molecular Basis of Heredity*, vol 29, pp. 107–126, Robert A. Welch Foundation, Houston, TX.

Berg, O. G. (1984). Diffusion-controlled protein-DNA association: influence of segmental diffusion of the DNA. *Biopolymers,* **23**, 1869–1889.

Chirico, G. & Langowski, J. (1992). Calculating hydro-dynamic properties of DNA through a second-order Brownian dynamics algorithm. *Macromolecules,* **25**, 769–775.

Chirico, G. & Langowski, J. (1994). Kinetics of DNA supercoiling studied by Brownian dynamic simulation. *Biopolymers,* **34**, 415–433.

Chirico, G. & Langowski, J. (1996). Brownian dynamic simulations of supercoiled DNA with bent sequences. *Biophys. J.* **71**, 955–971.

Ermak, D. L. & McCammon, J. A. (1978). Brownian dynamics with hydrodynamic interactions. *J. Chem. Phys.* **69**, 1352–1360.

Frank-Kamenetskii, M. D., Lukashin, A. V., Anshelevich, V. V. & Vologodskii, A. V. (1985). Torsional and bending rigidity of the double helix from data on small DNA rings. *J. Biomol. Struct. Dynam.* **2**, 1005–1012.

Gralla, J. D. (1996). Activation and repression of E. coli promoters. *Curr. Opin. Genet. Dev.* **6**, 526–530.

Hagerman, P. J. (1988). Flexibility of DNA. *Annu. Rev. Biophys. Biophys. Chem.* **17**, 265–286.

Hammermann, M., Stainmaier, C., Merlitz, H., Kapp, U., Waldeck, W., Chirico, G. & Langowski, J. (1997). Salt effects on the structure and internal dynamics of superhelical DNAs studied by light scattering and Brownian dynamic. *Biophys. J.* **73**, 2674–2687.

Heath, P. J., Gebe, J. A., Allison, S. A. & Schurr, J. M. (1996). Comparison of analytical theory with Brownian dynamics simulations for small linear and circular DNAs. *Macromolecules,* **29**, 3583–3596.

Hochschild, A. & Ptashne, M. (1986). Cooperative binding of lambda repressors to sites separated by integral turns of the DNA helix. *Cell,* **44**, 681–687.

Iniesta, A. & Garcia de la Torre, J. (1990). A 2nd-order algorithm for the simulation of the Brownian dynamics of macromolecular models. *J. Chem. Phys.* **92**, 2015–2018.

Jian, H., Vologodskii, A. & Schlick, T. (1997). Combined wormlike-chain and bead model for dynamic simulations of long linear DNA. *J. Comp. Phys.* **73**, 123–132.

Kanaar, R. & Cozzarelli, N. R. (1992). Roles of super-coiled DNA structure in DNA transactions. *Curr. Opion. Struct. Biol.* **2**, 369–379.

Langowski, J. & Giesen, U. (1989). Configurational and dynamic properties of different length superhelical DNAs measured by dynamic light scattering. *Biophys. Chem.* **34**, 9–18.

Marko, J. (1997). The internal 'slithering' dynamics of supercoiled DNA. *Physica sect. A,* **244**, 263–277.

Marko, J. F. & Siggia, E. D. (1995). Statistical mechanics of supercoiled DNA. *Phys. Rev. sect. E,* **52**, 2912–2938.

Menzel, R. & Gellert, M. (1994). The biochemistry and biology of DNA gyrase. *Advan. Pharmacol.* **29**, 39–69.

Oram, M., Marko, J. F. & Halford, S. E. (1997). Communications between distant sites on supercoiled DNA from non-exponential kinetics for DNA synapsis by resolvase. *J. Mol. Biol.* **270**, 396–412.

Parker, C. N. & Halford, S. E. (1991). Dynamics of long-range interactions on DNA: the speed of synapsis during site-specific recombination by resolvase. *Cell,* **66**, 781–791.

Peck, L. J. & Wang, J. C. (1981). Sequence dependence of the helical repeat of DNA in solution. *Nature,* **292**, 375–8.

Podtelezhnikov, A. & Vologodskii, A. (1997). Simulation of polymer cyclization by Brownian dynamics. *Macromolecules,* **30**, 6668–6673.

Rippe, K., von Hippel, P. H. & Langowski, J. (1995). Action at a distance: DNA-looping and initiation of transcription. *Trends Biochem. Sci.* **20**, 500–506.

Rotne, J. & Prager, S. (1969). Variational treatment of hydrodynamic interaction in polymers. *J. Chem. Phys.* **50**, 4831–4837.

Rybenkov, V. V., Vologoskii, A. V. & Cozzarelli, N. R. (1997a). The effect of ionic conditions on the confor-mations of supercoiled DNA. I. Sedimentation analysis. *J. Mol. Biol.* **267**, 299–311.

Rybenkov, V. V., Vologodskii, A. V. & Cozzarelli, N. R. (1997b). The effect of ionic conditions on the confor-mations of supercoiled DNA. II. Equilibrium catenation. *J. Mol. Biol.* **267**, 312–323.

Schleif, R. (1992). DNA looping. *Annu. Rev. Biochem.* **61**, 199–223.

Schlick, T. (1995). Modeling superhelical DNA: recent analytical and dynamic approaches. *Curr. Opin. Struct. Biol.* **5**, 245–262.

Schlick, T. & Olson, W. K. (1992). Supercoiled DNA energetics and dynamics by computer simulation. *J. Mol. Biol.* **223**, 1089–1119.

Schlick, T., Li, B. & Olson, W. K. (1994). The influence of salt on DNA energetics and dynamics. *Biophys. J.* **67**, 2146–2166.

Sessions, R. B., Oram, M., Szczelkun, M. D. & Halford, S. E. (1997). Random walk models for DNA synapsis by resolvase. *J. Mol. Biol.* **270**, 413–425.

Stark, W. M. & Boocock, M. R. (1995). Topological selectivity in site-specific recombination. In *Mobile Genetic Elements* (Sherratt, D. J., ed.), pp. 101–129, ARL PressOxford University Press, Oxford.

Stigter, D. (1977). Interactions of highly charged colloidal cylinders with applications to double-stranded DNA. *Biopolymers,* **16**, 1435–1448.

Tan, R. K. Z. & Harvey, S. C. (1989). Molecular mechanics model of supercoiled DNA. *J. Mol. Biol.* **205**, 573–591.

Tjian, R. & Maniatis, T. (1994). Transcriptional activation: a complex puzzle with few easy pieces. *Cell,* **77**, 5–8.

Vologodskii, A. V. (1992). *Topology and Physics of Circular DNA*, CRC Press, Boca Roton, FL.

Vologodskii, A. V. & Cozzarelli, N. R. (1994). Conformational and thermodynamic properties of super-coiled DNA. *Annu. Rev. Biophys. Biomol. Struct.* **23**, 609–643.

Vologodskii, A. V. & Cozzarelli, N. R. (1995). Modeling of long-range electrostatic interactions in DNA. *Biopolymers,* **35**, 289–296.

Vologodskii, A. V. & Cozzarelli, N. R. (1996). Effect of supercoiling on the juxtaposition and relative orientation of DNA sites. *Biophys. J.* **70**, 2548–2556.

Vologodskii, A. V., Levene, S. D., Klenin, K. V., Frank-Kamenetskii, M. D. & Cozzarelli, N. R. (1992). Conformational and thermodynamic properties of supercoiled DNA. *J. Mol. Biol.* **227**, 1224–1243.

Wang, J. C. (1996). DNA topoisomerases. *Annu. Rev. Biochem.* **65**, 635–695.

Wasserman, S. A. & Cozzarelli, N. R. (1986). Biochemical topology: applications to DNA recombination and replication. *Science,* **232**, 951–960.

Wilemski, G. & Fixman, M. (1974). Diffusion-controlled intrachain reactions of polymers. II. Results for a pair of terminal reactive groups. *J. Chem. Phys.* **60**, 878–890.

Edited by I. Tinoco